Topological Charge Pumping in a One-Dimensional Optical Lattice

Lei Wang,[1,2] Matthias Troyer,[1] and Xi Dai[2]

[1]*Theoretische Physik, ETH Zurich, 8093 Zurich, Switzerland*

[2]*Beijing National Lab for Condensed Matter Physics and Institute of Physics, Chinese Academy of Sciences, Beijing 100190, China*

(Received 30 January 2013; published 9 July 2013)

A topological charge pump transfers charge in a quantized fashion. The quantization is stable against the detailed form of the pumping protocols and external noises and shares the same topological origin as the quantum Hall effect. We propose an experimental setup to realize topological charge pumping of cold fermionic atoms in a one-dimensional optical lattice. The quantization of the pumped charge is confirmed by first-principles simulations of the dynamics of uniform and trapped systems. Quantum effects are shown to be crucial for the topological protection of the charge quantization. Finite-temperature and nonadiabatic effects on the experimental observables are discussed. The realization of such a topological charge pump serves as a firm step toward exploring topological states and nonequilibrium dynamics using cold atoms.

DOI: 10.1103/PhysRevLett.111.026802 PACS numbers: 73.43.−f, 03.65.Vf, 67.85.Lm

Introduction.—Charge pumping is a standard method to generate a steady current in solid-state circuits [1–5] through adiabatically and periodically time-varying potentials. The effect bears a similarity to the famous Archimedes screw [6], where water is pumped by a rotating spiral tube. However, quantum physics offers a more intriguing phenomenon: quantum charge pumping, where the charge transferred in each pumping cycle is exactly quantized. Thouless [1] has shown that the one-dimensional (1D) quantum charge pump shares the same topological origin as the two-dimensional (2D) quantum Hall effect (QHE) [7]. The amount of pumped charge can be expressed by the Chern number of a 2D QHE Hamiltonian [8]. In other areas of condensed matter physics, the theory of quantized charge pumping also lays a firm foundation for the modern theory of polarization of crystalline solids [9,10], the theory for Z_2 spin pump [11,12], and inspired the theoretical connection [13] between the 3D Z_2 topological insulators and the 4D quantum Hall effect [14]. The word *quantum* in the quantum charge pumping has twofold meanings. First, the pumped charge is quantized. Second, one actually relies on the quantum mechanics (thus, the concept of Berry phase and energy gap) for the topological protection of the quantized charge.

A clean and highly tunable cold atom system provides an opportunity to realize and detect this topological charge pumping effect. Specifically, advances in constructing optical superlattice structure [15–17] and nonequilibrium control of lattice intensity and phases [18] allow the realization of a charge pumping setup, which we will propose in this Letter. *In situ* detection with the single-site resolution [19–21] allows the detection of topological charge pumping. The equivalence of 1D topological charge pumping and the 2D quantum Hall effect connects our proposal to recent efforts of exploring topological quantum phases with synthetic gauge field [22–25] and spin-orbit couplings [26–28], where one of the landmarks is to realize the quantum Hall effect [7] and topological insulator [29] state in atomic quantum gases.

In this Letter, we consider the topological charge pumping of cold fermions in a 1D optical lattice potential. First, we show that the proposed potential indeed realizes the topological charge pumping by calculating its Chern number and *ab initio* simulation of the pumping process. Compared with the corresponding classical dynamics, we show that quantum effects are crucial for the topological protection of the quantized charge pumping. We then consider the effect of a harmonic trap and predict the topological quantization of the center of mass of the cloud in realistic experimental situations.

Our proposal is based on a time-dependent 1D optical superlattice of the form [15–18]

$$V_{\mathrm{OL}}(x,t) = V_1\cos^2\left(\frac{2\pi x}{d}\right) + V_2\cos^2\left(\frac{\pi x}{d} - \varphi(t)\right). \quad (1)$$

We use the lattice constant d as the unit of length and the recoil energy $E_R = (\hbar^2\pi^2/2md^2)$ as the unit of energy, where m is the mass of the atom. Such superlattices have been experimentally realized in Refs. [15–18]. The lattice strengths V_1 and V_2 and the phase factor φ can be tuned dynamically.

We propose to vary the relative phase linearly with time

$$\varphi(t) = \frac{\pi t}{T}. \quad (2)$$

The lattice then changes in time with a period T. In the absence of the static short wavelength lattice controlled by the V_1 term, the V_2 term describes a sliding lattice shown in Fig. 1(a). Including the V_1 term, one realizes the Rice-Mele model [30] in a continuous space setup, as illustrated in Figs. 1(b) and 1(c). This can easily be seen by expanding the V_2 term (neglecting spatially independent constants)

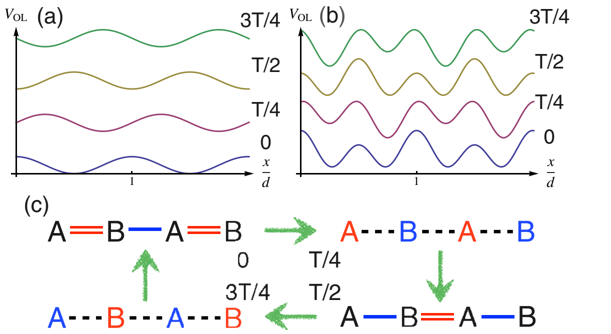

FIG. 1 (color online). Two topological equivalent pumping lattices. (a) A sliding lattice ($V_1 = 0$, $V_2 = 1E_R$) (b) A continuous Rice-Mele pump [30] ($V_1 = 2E_R$, $V_2 = 1E_R$), where the dimerization of hopping amplitudes and on-site energies is modulated periodically. At $t = 0$ and $t = T/2$, different topological phases of the Su-Schrieffer-Heeger lattice [31] are realized. (c) A tight-binding schematic view of the pumping process in (b). The two pumping processes (a) and (b) are topologically equivalent for the lowest band and can be adiabatically connected; see the main text.

into two oscillating terms individually controlling the dimerized hopping amplitudes and the sublattice energy offsets:

$$V_2 \cos\left(\frac{2\pi t}{T}\right)\cos^2\left(\frac{\pi x}{d}\right) + V_2 \sin\left(\frac{2\pi t}{T}\right)\cos^2\left(\frac{\pi x}{d} - \frac{\pi}{4}\right). \quad (3)$$

At time $t = 0$ and $t = T/2$, only the first term is nonzero, realizing the Su-Schrieffer-Heeger (SSH) model [31]. This model exhibits two topologically distinguishable phases which are protected by inversion symmetry. The second term of Eq. (3) breaks this inversion symmetry and smoothly connects the two phases of the SSH model. At $t = T/4$, the system has uniform hopping amplitude but different on-site energies at two sublattices. At $t = T/2$, the system enters a different topological phase of the SSH model than at $t = 0$. Since the gap of the Hamiltonian does not close during the pumping process, we can define a topological index associated with the pumping process. This index is just the Chern number of a 2D QHE Hamiltonian and gives the charge pumped during one cycle. The continuum potential Eq. (1) interpolates between the sliding potential and the Rice-Mele model. They are topologically equivalent since one could adiabatically switch on the V_1 term without closing the gap [32].

Infinite system.—We first consider topological charge pumping of spinless fermions in an infinite periodic system with Hamiltonian

$$H(x, t) = -\frac{\hbar^2}{2m}\nabla^2 + V_{\mathrm{OL}}(x, t). \quad (4)$$

There are several advantages to working with a continuum model instead of a tight-binding lattice model like in Ref. [33]. Continuum models apply to a broader range of experimental situations, including shallow optical lattices. Multiband effects are fully included in our calculations [34]. A continuum model also allows us to directly compare with classical pumping dynamics and to demonstrate the importance of quantum effects for the topological protection of the pumped charge.

Figure 2(a) shows the spatial-temporal structure of $V_{\mathrm{OL}}(x, t)$ for $V_1 = V_2 = 4E_R$, which we will refer to as the Rice-Mele pumping potential in the following. Performing a Fourier transform of $H(x, t)$, we obtain the Bloch Hamiltonian $H(k_x, t)$, which satisfies the periodicity conditions $H(k_x + 2\pi, t) = H(k_x, t)$ and $H(k_x, t + T) = H(k_x, t)$. Since there is always a gap to higher bands, we can calculate the Chern number of the lowest band of $H(k_x, t)$ as if it was a two-dimensional Hamiltonian [35,36]. Figure 2(b) shows the Berry curvature distribution in the $k_x - t$ space. Integration of the Berry curvature over the Brillouin zone shows that the Chern number is equal to 1.

Thouless showed [1] that at zero temperature under the adiabatic approximation, the pumped charge equals the Chern number for a filled band. We now proceed to simulate the pumping process and directly calculate the pumped charge. For an infinite system, the pumped charge is defined through the integration of the total current (see the Supplemental Material for details [37]):

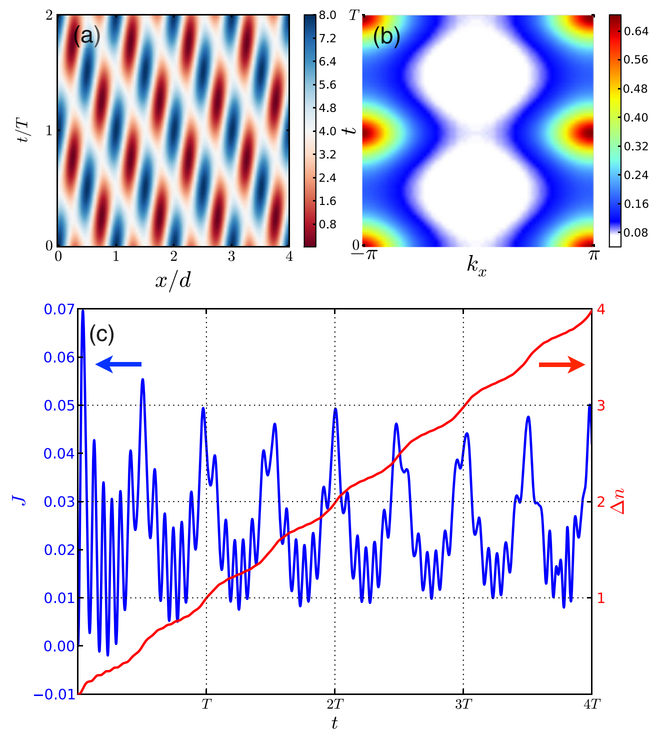

FIG. 2 (color online). (a) Spatial-temporal structure of the optical lattice Eq. (1) for $V_1 = V_2 = 4E_R$. (b) Berry curvature distribution of the lowest band of $H(k_x, t)$. Integration over the Brillouin zone shows the Chern number equals 1. (c) Pumped charge and total current Eq. (5) of an infinite-sized system with $T = 40\hbar/E_R$ and one particle per unit cell. The pumped charge is quantized at full pumping cycles.

$$\Delta n(t) = \int_0^t dt' J(t'). \tag{5}$$

Figure 2(c) shows the current and pumped charge for pumping cycle $T = 40\hbar/E_R$ in the Rice-Mele pumping potential (the band gap is $\sim 1.5E_R$). The sudden onset of pumping causes high frequency oscillations of the current. The pumped charge is quantized at times that are multiples of the cycle time T. Our calculations show that modifying the quantum pump by changing V_1 and V_2 results in a different current $J(t)$; however, the pumped charge remains quantized. One thus realizes a topological pump, neither relying on a tight-binding approximation nor the details of the pumping protocol.

Figure 3 shows nonadiabatic and finite-temperature effects on the quantization of pumped charge. Quantization is precise for slow pumping and low temperature compared to the band gap. Considering ^{40}K atoms and $d = 532$ nm, one has $\hbar/E_R = 36.4\ \mu$s and $E_R/k_B = 0.21\ \mu$K. Thus, for a pumping period longer than $50\hbar/E_R \approx 2$ ms and initial temperature lower than $0.1E_R/k_B \approx 20$ nK, the pumped charge is quantized to within 0.2%. Such a pump is feasible within current experimental abilities.

To demonstrate the importance of quantum mechanics for topological protection, we examine classical pumping in the same lattice potential. For a sliding lattice ($V_1 = 0$, $V_2 = 4E_R$), both the quantum and classical pump transfer units charge in one cycle. However, mapping the classical problem to a classical pendulum (see the Supplemental Material [37]) shows that this is accidental, and the pumped charge is not exactly quantized. This accidental quantization is removed by changing the atom mass, the lattice constant, or the pumping potential. Figure 3 shows that the pumped charge drops to close to zero for the classical Rice-Mele pump at low temperature. It is because of the potential minima felt by the classical particle does not shift in space. On the contrary, the quantization in the quantum case is protected by an energy gap and survives as one distorts the pumping potential to the Rice-Mele model. The difference between classical and quantum behavior is due to the absence of Berry phases and energy gaps in classical dynamics. This comparison highlights the importance of quantum effects for topological protection.

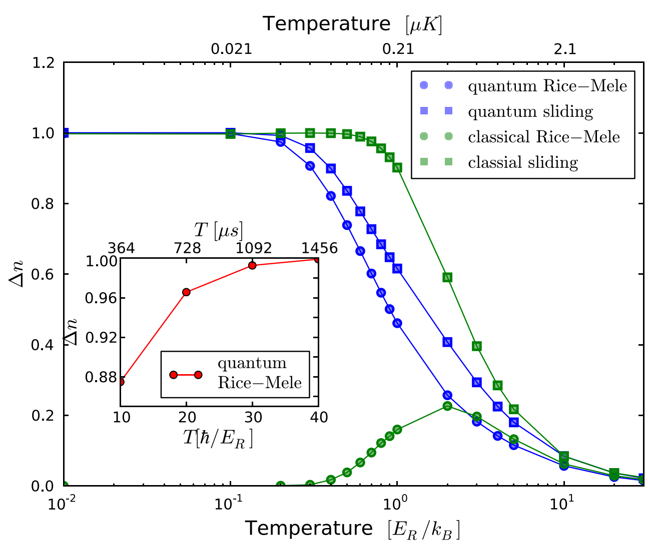

FIG. 3 (color online). The pumped charge after one cycle vs temperature for the quantum and classical case. Quantization of the pumped charge is visible for temperature lower than the band gap. For the classical case, there is no such topological protection and the pumped charge depends on the pumping protocols. The inset shows the nonadiabatic (finite-pumping time) effect on the pumped charge of a quantum Rice-Mele pump. The upper axis shows the realistic temperature and time estimated for ^{40}K atoms in a $d = 532$ nm laser.

At finite temperatures, quantization in the quantum pump remains stable for temperature smaller than the energy gap (see Fig. 3). The quantum to classical transition is determined by the condition $n\lambda \ll 1$, where $\lambda = \hbar\sqrt{2\pi\beta/m}$ is the thermal de Broglie wavelength, β is the inverse temperature, and n is the average density of the system. Classical behavior dominates when $\beta^{-1} \gg (4(nd)^2/\pi)E_R$. For a shallow optical lattice $nd \sim 1$, the quantum to classical crossover happens at temperatures much larger than E_R. For ^{40}K atoms and $d = 532$ nm, the whole temperature region of the quantum to classical crossover in Fig. 3 can be achieved in experiments.

Trapped system.—To connect to real experimental situations, we link the quantization to a simple physical observable: the center of mass of a cloud in a harmonic trap $V_{\text{trap}}(x) = (1/2)m\omega_T^2 x^2$, which varies slowly compared to the optical lattice. In Fig. 4(a), we show the initial

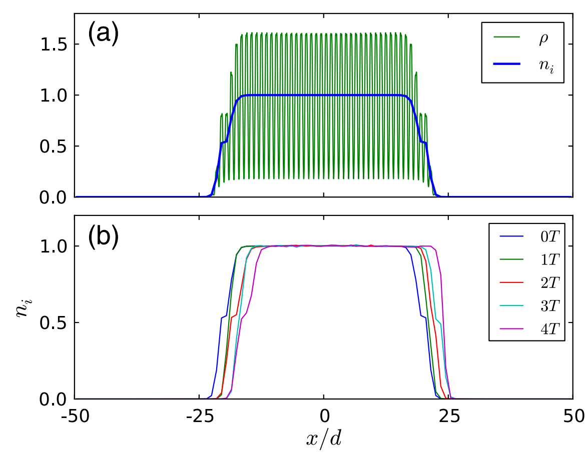

FIG. 4 (color online). (a) Initial density distribution in a harmonic trap with $\omega_T = 0.03E_R$, $V_1 = V_2 = 4E_R$, and particle number $N = 40$. The green curve shows the continuous space density, while the blue curve shows the occupation number integrated over each unit cell. (b) Occupation number after several cycles of pumping with $T = 40\hbar/E_R$, time increases from left to right. The cloud shifts to the right, and the center of mass position is quantized; see Fig. 5.

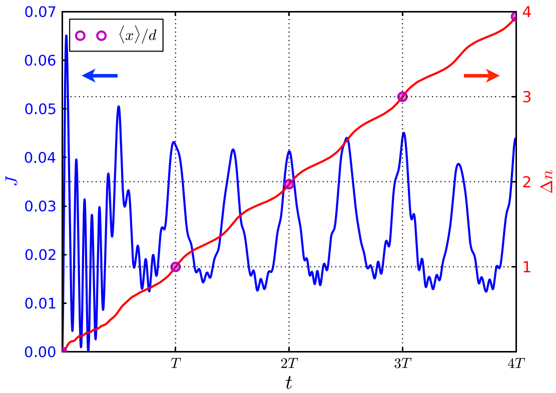

FIG. 5 (color online). Total current (blue line), pumped charge (red line), and center of mass (pink circles) of the atomic cloud in a harmonic trap. The c.m. shift is equal to the pumped charge and is quantized at integer cycles. The pumping parameters are the same as in Fig. 4.

ground-state density distribution $\rho(x, t = 0)$ in a trap with frequency $\omega_T = 0.03E_R$. In order to clearly see the nature of the state of trapped gas, we integrate the density over each unit cell, arriving at site occupations

$$n_i(t) = \int_{\Omega_i} dx \rho(x, t), \tag{6}$$

which are show as blue lines in Fig. 4(a). We see a band insulator ($n_i = 1$) in the center of the trap with very small metallic wings.

Calculating the time evolution, we show in Fig. 4(b) the occupation number after multiple pumping cycles for $V_1 = V_2 = 4E_R$ and $T = 40\hbar/E_R$. We observe that the cloud shifts to the right under the action of the pump. To reveal the topological nature of this drift, we show that the center of mass (c.m.) of the cloud

$$\langle x(t) \rangle = \frac{1}{N} \int_{-\infty}^{\infty} dx \rho(x, t) x \tag{7}$$

encodes the topological pumped charge Δn

$$\langle x \rangle / d = \Delta n. \tag{8}$$

Equation (8) links the pumped charge Δn with the physical observables $\langle x \rangle$. Experimentally, the c.m. position $\langle x \rangle$ can be measured precisely, either by *in situ* measurement of the density distribution or deduced indirectly from time-of-flight imaging [38,39]. The topological pumping effect can then be identified as a quantization of c.m. position at multiple pumping cycles. To proof Eq. (8), we multiply x to both sides of the continuity equation and then integrate over spacetime, noticing that the current dies out at infinity for a trapped system.

Figure 5 shows the total current J, pumped charge Δn, and c.m. $\langle x \rangle$ in a trap. The relationship Eq. (8) is evident from the plot, and we clearly see quantization of the pumped charge and c.m. at every full pumping cycle. The similarities between Figs. 2 and 5 show that the external trap and finite size of the atomic cloud do not affect the precise quantization of the pumped charge. The observation of this effect in cold atom systems is thus highly feasible, with *in situ* imaging techniques for the atomic cloud [19–21].

Finite-size effects and metallic edges will, in principle, give a nonquantized value of the pumped charge. Any such deviation from an integer value is, however, not visible in our simulations and will be even smaller in the experimental situation where the trap is larger and finite-size effects are thus smaller. While topological pumping is stable against weak interactions [40], interaction effects can also easily be avoided by using spin-polarized atoms.

Conclusion.—We have proposed a realistic experimental setup to realize the topological pumping of cold atoms. Our setup naturally interpolates between sliding potentials and the Rice-Mele model [30] commonly studied in condensed matter physics. The quantization of the pumped charge can be observed from a quantization of the center of mass motion of the atomic cloud, is independent of the details of the pumping protocol, and is robust with respect to nonzero temperature. The experimental observation of topological pumping in cold atoms will be a big step toward exploring topological states and nonequilibrium dynamics in cold atom systems.

As further steps, interactions on a fractionally occupied lattice may open up an energy gap, and one could pump a fractional charge in each pumping cycle. With two spin species, it will be interesting to see Z_2 spin pumping where the Wannier centers of two time-reversal-symmetrical states split and exchange [12,41].

This work is supported by the Swiss National Science Foundation through the NCCR QSIT and the European Research Council. X. D. is supported by the National Science Foundation of China. We thank Thomas Uehlinger, Jean-Philippe Brantut, Ulrich Schneider, and Christian Gross for helpful discussions. The simulations were performed on the Brutus Cluster at ETH Zurich.

[1] D. J. Thouless, Phys. Rev. B **27**, 6083 (1983).
[2] J. M. Shilton, V. I. Talyanskii, M. Pepper, D. A. Ritchie, J. E. F. Frost, C. J. B. Ford, C. G. Smith, and G. A. C. Jones, J. Phys. Condens. Matter **8**, L531 (1996).
[3] M. Switkes, C. M. Marcus, K. Campman, and A. C. Gossard, Science **283**, 1905 (1999).
[4] M. D. Blumenthal, B. Kaestner, L. Li, S. R. Giblin, T. J. B. M. Janssen, M. Pepper, D. Anderson, G. Jones, and D. A. Ritchie, Nat. Phys. **3**, 343 (2007).
[5] B. Kaestner, V. Kashcheyevs, S. Amakawa, M. D. Blumenthal, L. Li, T. J. B. M. Janssen, G. Hein, K. Pierz, T. Weimann, U. Siegner, and H. W. Schumacher, Phys. Rev. B **77**, 153301 (2008).

[6] B.L. Altshuler and L.I. Glazman, Science **283**, 1864 (1999).

[7] K. Klitzing, G. Dorda, and M. Pepper, Phys. Rev. Lett. **45**, 494 (1980).

[8] D.J. Thouless, M. Kohmoto, M.P. Nightingale, and M. den Nijs, Phys. Rev. Lett. **49**, 405 (1982).

[9] R.D. King-Smith and D. Vanderbilt, Phys. Rev. B **47**, 1651 (1993).

[10] R. Resta, Rev. Mod. Phys. **66**, 899 (1994).

[11] R. Shindou, J. Phys. Soc. Jpn. **74**, 1214 (2005).

[12] L. Fu and C.L. Kane, Phys. Rev. B **74**, 195312 (2006).

[13] X.-L. Qi, T.L. Hughes, and S.-C. Zhang, Phys. Rev. B **78**, 195424 (2008).

[14] S.-C. Zhang and J. Hu, Science **294**, 823 (2001).

[15] S. Peil, J.V. Porto, B. Laburthe Tolra, J.M. Obrecht, B.E. King, M. Subbotin, S.L. Rolston, and W.D. Phillips, Phys. Rev. A **67**, 051603 (2003).

[16] S. Fölling, S. Trotzky, P. Cheinet, M. Feld, R. Saers, A. Widera, T. Müller, and I.F. Bloch, Nature (London) **448**, 1029 (2007).

[17] S. Trotzky, P. Cheinet, S. Foelling, M. Feld, U. Schnorrberger, A.M. Rey, A. Polkovnikov, E.A. Demler, M.D. Lukin, and I.F. Bloch, Science **319**, 295 (2008).

[18] M. Atala, M. Aidelsburger, J.T. Barreiro, D. Abanin, T. Kitagawa, E. Demler, and I. Bloch, arXiv:1212.0572v1.

[19] W.S. Bakr, A. Peng, M.E. Tai, R. Ma, J. Simon, J.I. Gillen, S. Folling, L. Pollet, and M. Greiner, Science **329**, 547 (2010).

[20] J.F. Sherson, C. Weitenberg, M. Endres, M. Cheneau, I.F. Bloch, and S. Kuhr, Nature (London) **467**, 68 (2010).

[21] C. Weitenberg, M. Endres, J.F. Sherson, M. Cheneau, P. Schauß, T. Fukuhara, I.F. Bloch, and S. Kuhr, Nature (London) **471**, 319 (2011).

[22] Y.J. Lin, R.L. Compton, K. Jiménez-García, J.V. Porto, and I.B. Spielman, Nature (London) **462**, 628 (2009).

[23] M. Aidelsburger, M. Atala, S. Nascimbène, S. Trotzky, Y.A. Chen, and I. Bloch, Phys. Rev. Lett. **107**, 255301 (2011).

[24] J. Struck, C. Ölschläger, M. Weinberg, P. Hauke, J. Simonet, A. Eckardt, M. Lewenstein, K. Sengstock, and P. Windpassinger, Phys. Rev. Lett. **108**, 225304 (2012).

[25] K. Jimenez-Garcia, L.J. LeBlanc, R.A. Williams, M.C. Beeler, A.R. Perry, and I.B. Spielman, Phys. Rev. Lett. **108**, 225303 (2012).

[26] Y.J. Lin, K. Jimenez-Garcia, and I.B. Spielman, Nature (London) **471**, 83 (2011).

[27] P. Wang, Z.-Q. Yu, Z. Fu, J. Miao, L. Huang, S. Chai, H. Zhai, and J. Zhang, Phys. Rev. Lett. **109**, 095301 (2012).

[28] L.W. Cheuk, A.T. Sommer, Z. Hadzibabic, T. Yefsah, W.S. Bakr, and M.W. Zwierlein, Phys. Rev. Lett. **109**, 095302 (2012).

[29] M.Z. Hasan and C.L. Kane, Rev. Mod. Phys. **82**, 3045 (2010).

[30] M.J. Rice and E.J. Mele, Phys. Rev. Lett. **49**, 1455 (1982).

[31] W.P. Su, J.R. Schrieffer, and A.J. Heeger, Phys. Rev. Lett. **42**, 1698 (1979).

[32] This equivalence is only limited to the lowest band since the band gap between higher bands closes.

[33] Y. Qian, M. Gong, and C. Zhang, Phys. Rev. A **84**, 013608 (2011).

[34] M. Modugno and G. Pettini, New J. Phys. **14**, 055004 (2012).

[35] D. Xiao, M.-C. Chang, and Q. Niu, Rev. Mod. Phys. **82**, 1959 (2010).

[36] T. Fukui, Y. Hatsugai, and H. Suzuki, J. Phys. Soc. Jpn. **74**, 1674 (2005).

[37] See Supplemental Material at http://link.aps.org/supplemental/10.1103/PhysRevLett.111.026802 for detailed descriptions about the simulation methods and the classical pumping dynamics.

[38] C.D. Fertig, K.M. O'Hara, J.H. Huckans, S.L. Rolston, W.D. Phillips, and J.V. Porto, Phys. Rev. Lett. **94**, 120403 (2005).

[39] N. Strohmaier, Y. Takasu, K. Günter, R. Jördens, M. Köhl, H. Moritz, and T. Esslinger, Phys. Rev. Lett. **99**, 220601 (2007).

[40] Q. Niu and D.J. Thouless, J. Phys. A **17**, 2453 (1984).

[41] R. Yu, X.-L. Qi, A. Bernevig, Z. Fang, and X. Dai, Phys. Rev. B **84**, 075119 (2011).